Surface Segregation of Dissolved Salt Ions

Oliver Höfft,[†] Andriy Borodin,[†,||] Uwe Kahnert,[†] Volker Kempter,*[,†] Liem X. Dang,[‡] and Pavel Jungwirth*[,§]

Technische Universität Clausthal, Institut für Physik und Physikalische Technologien, Leibnizstr. 4, D-38678 Clausthal-Zellerfeld, Germany, Chemical Sciences Division, Pacific Northwest National Laboratory, Richland, Washington 99352, U.S.A., and Institute of Organic Chemistry and Biochemistry, Academy of Sciences of the Czech Republic, and Center for Biomolecules and Complex Molecular Systems, Flemingovo nám. 2, 16610 Prague 6, Czech Republic

Received: March 8, 2006

Surface segregation of iodide, but not of fluoride or cesium ions, is observed by a combination of metastable impact electron spectroscopy (MIES) and ultraviolet photoelectron spectroscopy (UPS(HeI)) of amorphous solid water exposed to CsI or CsF vapor. The same surface ionic behavior is also derived from molecular dynamics (MD) simulations of the corresponding aqueous salt solutions. The MIES results show the propensity of iodide, but not fluoride, for the surface of the amorphous solid water film, providing thus strong evidence for the suggested presence of heavier halides (iodide, bromide, and to a lesser extent chloride) at the topmost layer of aqueous surfaces. In contrast, no appreciable surface segregation of ions is observed in methanol, neither in the experiment nor in the simulation. Furthermore, the present results indicate that, as far as the thermodynamic aspects of solvation of alkali halides are concerned, amorphous solid water and methanol surfaces behave similarly as surfaces of the corresponding liquids.

Introduction

Penetration of atoms, molecules, or ions through the surface of aqueous or ice-like matter and, conversely, the segregation of these species from the bulk to the surface is involved in many natural and technological processes.[1] In a polar medium such as water, ions are ubiquitous and can actively participate in the segregation phenomena. Electrostatic forces, however, repel ions from the surface into the aqueous bulk.[2] Therefore, according to common wisdom, only large hydrophobic ions (e.g., containing a hydrocarbon chain or ring) can segregate to the surface, whereas surfaces of simple salt solutions are devoid of ions.[3,4] This textbook picture has been recently confronted with molecular dynamics simulations indicating that heavier halides, i.e., iodide, bromide, and to some extent also chloride, exhibit a propensity for the air/water interface.[5−9]

Due to their fundamental novelty, as well as implications for heterogeneous atmospheric chemistry,[5,10,11] the theoretical predictions have been challenged by various surface-selective experiments. In general, second harmonic generation (SHG),[12] vibrational sum frequency generation (VSFG),[13,14] and high-pressure photoelectron spectroscopy (PES) measurements[15,16] support the theoretical predictions. Nevertheless, none of the above techniques provides information solely about the topmost layer, but they all, to a varying extent, average over the interfacial region. Obtaining detailed molecular information for liquid surfaces is inherently much more difficult than for solids, due to the high mobility, disorder, and volatility of the former environment. The importance of the results of computer simulations concerning the surface propensity of heavier halides, as well as the persisting ambiguities, were stressed recently, and it was stated explicitly that "if true, atmospheric scientists may have to ponder new types of chemical reactions occurring on the surface of aerosol particles".[17]

In this situation, it is fortunate that a solid-state analogue to liquid water, namely the amorphous solid water (ASW), exists for which straightforward and detailed surface-sensitive experiments can be performed. Water vapor deposited on a surface at low temperatures in a vacuum forms an amorphous solid. ASW has a glass transition temperature around $T_g = 135$ K.[1,18,19] Above T_g, ASW is a viscous liquid which undergoes a kinetic phase transition to cubic crystalline ice above ∼140 K. ASW is structurally very similar to water, whereas it is closer to ice in its dynamical properties (diffusion).[19] Finally, water is not the only polar medium that can be prepared in an amorphous solid phase, another example being methanol,[20] which together with ASW represents an important component of the interstellar matter.[19]

A natural question arises as to whether the surface propensity of heavier halides predicted in the aqueous environment is, if true, a general property of polar media or whether it is pertinent to water. Here, we address this question by a combination of metastable impact electron spectroscopy (MIES) and ultraviolet photoelectron spectroscopy UPS(HeI) experiments on amorphous solid water and methanol exposed to CsI or CsF vapor and molecular dynamics simulations of the corresponding liquid solutions. To this end, we apply the combination of MIES and UPS(HeI) to the study of the interaction of CsI with both water and methanol between 100 and 170 K. The measurements for CsI are directly compared with corresponding results obtained for cesium fluoride[21] and can be also related to very recent low-energy sputtering (LES) studies for NaCl on amorphous ice

* To whom correspondence should be addressed. E-mail: V.Kempter@tu-clausthal.de (V.K.) and Pavel.Jungwirth@uochb.cas.cz (P.J.).
† Institut für Physik und Physikalische Technologien.
‡ Pacific Northwest National Laboratory.
§ Academy of Sciences of the Czech Republic.
|| Present address: Dept. Chemistry, Graduate School of Science, Tohoku University, Aoba-ku, Sendai 980-8578, Japan.

10.1021/jp061437h CCC: $33.50
Published on Web 04/20/2006

films, indicating the inward motion of Na^+ when increasing the ice temperature beyond about 120 K, in contrast to the near-surface residence of Cl^-.[22] The choice of cesium salts allows to follow the release of the uppermost p-electron of the cation (5pCs) by means of MIES and UPS(HeI), which would not be possible for any other alkali cation.

Experimental Section

Properties and Characterization of Amorphous Solid Water. ASW is formed during the slow deposition of water vapor at temperatures below 120 K, typically.[1,23] Deposition below 80 K results in the formation of a microporous structure, responsible for the gas adsorption at very low temperatures. By annealing, ASW is thought to convert into a viscous-liquid phase above its glass transition temperature (136 K). This is followed by crystallization.

Around 120−125 K, the rotational relaxation of hydrogen-bond defects is believed to become important. This allows for the surface and near-surface gas adsorption on ASW films. Above 135 K, the translational diffusion of H_2O molecules becomes important (on the time scale of typical experiments). This leads to the bulk incorporation of adsorbates. When annealing above 140 K, imperfections of the water-hydrogen bonds are healed out efficiently, and as a consequence, the incorporation of gas adsorbates into the bulk becomes inhibited. On the other hand, due to the efficient surface diffusion of H_2O molecules, partial hydration of adsorbates still occurs under these conditions by the formation of a surface complex.

Experimental Details. The apparatus, applied to the study of salt−ASW and salt−amorphous solid methanol, has been described in detail previously.[21,24] A cold-cathode gas-discharge source produces metastable He* atoms ($He2^3S/2^1S$ ratio of 7:1 and excitation energies of 19.8/20.6 eV, respectively) for MIES and HeI photons (21.2 eV) as a source for UPS. He* metastables with thermal kinetic energy (60−100 meV) approach the surface; therefore, this technique is nondestructive and highly surface sensitive (see refs 25 and 26 for a more detailed introductions into MIES and its various applications in molecular and surface spectroscopy). The spectral contributions from metastables and photons are separated be means of a time-of-flight technique. Electrons emitted by He* atoms and UV photons are analyzed in the direction normal to the surface using a hemispherical analyzer.

The support (polycrystalline Au) can be cooled with liquid nitrogen to 100 K. It is exposed to water or methanol by backfilling the chamber. The exposures are stated in Langmuirs (L) ($1\ L = 10^{-6}$ Torr · s). On the basis of previous results, we estimate that 4 L correspond to ∼1 bilayer of water. To anneal the prepared films, their temperature is ramped slowly (1 K/min, resulting in a different desorption temperature as compared to TPD). The time required to collect a pair of MIES and UPS spectra quasi-simultaneously is about 60 s. CsI was deposited by evaporating polycrystalline salt at ∼700 K. Our previous results for salt adsorption on metals (tungsten) indicate a work-function decrease until a surface coverage of 0.5 monolayer is reached.

Computational Methods

The aqueous solution/vapor interface was modeled by 1 ns molecular dynamics simulations (after 500 ps of equilibration) of water slabs containing CsF at ∼1.2 M or CsI at ∼1.2 or ∼3 M concentration. Simulations in slab geometry were performed using the AMBER 6 program[27] using polarizable potentials both for water (POL3)[28] and the dissolved ions.[7,29−30] The induced electric field was converged in each step using a self-consistent procedure.

A slab of 864 water molecules was used to construct each system by adding 18 (or 48) cations and 18 (or 48) anions for the ∼1.2 M (or ∼3 M) solution. Each slab was placed into a $30 \times 30 \times 100$ Å^3 rectangular box, and periodic boundary conditions were applied in all three dimensions. The simulations were run at a constant temperature of 300 K. The smooth particle mesh Ewald method[31] was used to calculate the long-range electrostatic energies and forces, and the van der Waals interactions and the real space part of the Ewald sum were truncated at 12 Å. A time step of 1 fs was used in the integration of the equations of motion, with the water OH bonds frozen using the SHAKE algorithm.[32]

Simulations of the methanol solution/vapor interface were performed in a unit cell of $32 \times 32 \times 135$ Å^3 containing 875 methanol molecules and 18 cesium and iodide ions. The methanol force field was the same as in our previous study.[33] All other simulation conditions were the same as in the water simulations.

Results and Discussion

Experimental Results. In MIES, metastable He atoms of thermal energy interact via Auger processes solely with the species at the surface.[25,26] The ejected electrons thus bear information on the electronic structure of the surface topmost layer exclusively. For this reason, MIES (in combination with UPS(HeI), which probes a somewhat thicker region of several layers[15,16]) is well suited for the study of surface solvation and segregation processes, such as those occurring during the interactions of halide salts with amorphous solid water or methanol.

The signatures of salt ions and water in the MIES and UPS spectra follow from previous combined MIES/UPS results for cesium halide films on tungsten and on ASW.[21] Peaks are seen from the ionization of 5pCs (at 11.5 and 13 eV for $5p_{(3/2)}$Cs and $5p_{(1/2)}$Cs, respectively) and the valence p-orbital of the halide (at 7.2, 5.5, and 4.7 eV for F, Cl, and I, respectively). Water exposure between 80 and 130 K produces the three valence features $1b_1$, $3a_1$, and $1b_2$,[21] seen both with MIES and UPS (at 7.5, 9.8, and 12.9 eV). All energies are with respect to the Fermi level of the metal support. Methanol exposure in the same temperature range produces five spectral features M_1-M_5. According to refs 24 and 34, M_1-M_5 have a $n_{O\perp}$, $n_{O\parallel}$, σ_{CO}, π_{CO}, and σ_{OH} character, respectively.

Figures 1 and 2 present MIES and UPS results for CsI interacting with ASW and amorphous solid methanol. An ASW film (10 layers, typically), held at 100 K, is exposed to CsI molecules. This produces the spectral structure I(5p) due to ionization to the two iodine fine-structure states $5p_{1/2}$ and $5p_{3/2}$ (typically at energies of 3.5 and 4.5 eV, respectively). The curves indicate how the position of I(5p) changes slightly with temperature. The expected analogous structure from the ionization of the Cs(5p) fine-structure states is partially obscured by the strong emission from the H_2O $3a_1$ and $1b_2$ states. The change of the I(5p) intensity with temperature, as seen with MIES, is displayed in Figure 3, together with the corresponding variation of the $1b_1$ H_2O and $M_{3,4}$ methanol signals (for the calibration of the I(5p) signals obtained for ASW and amorphous solid methanol relative to each other, see later in this section).

Upon annealing the surface, we see for ASW first an increase of the H_2O-induced signals, correlated with a decrease of I(5p)

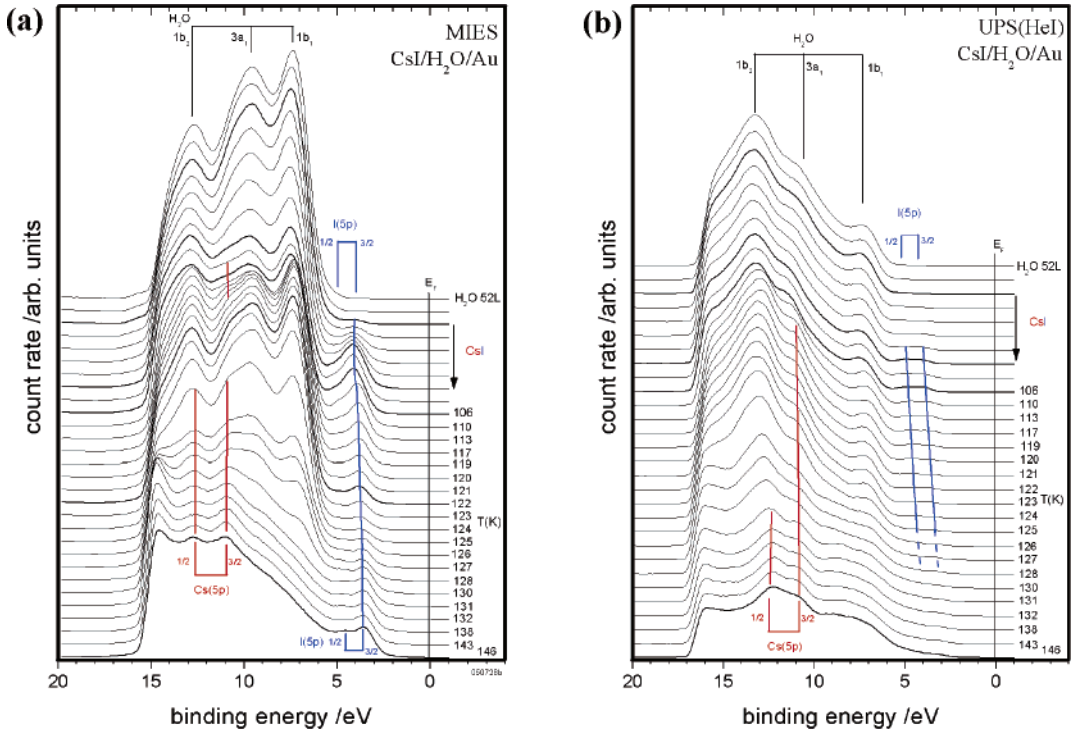

Figure 1. (a) MIES and (b) UPS(HeI) spectra for CsI interacting with amorphous solid water (ASW). Shown are the spectra of the ASW film prior and after the CsI deposition at about 100 K (upper part) and during the variation of the temperature of the ASW film between 106 and 146 K (lower part).

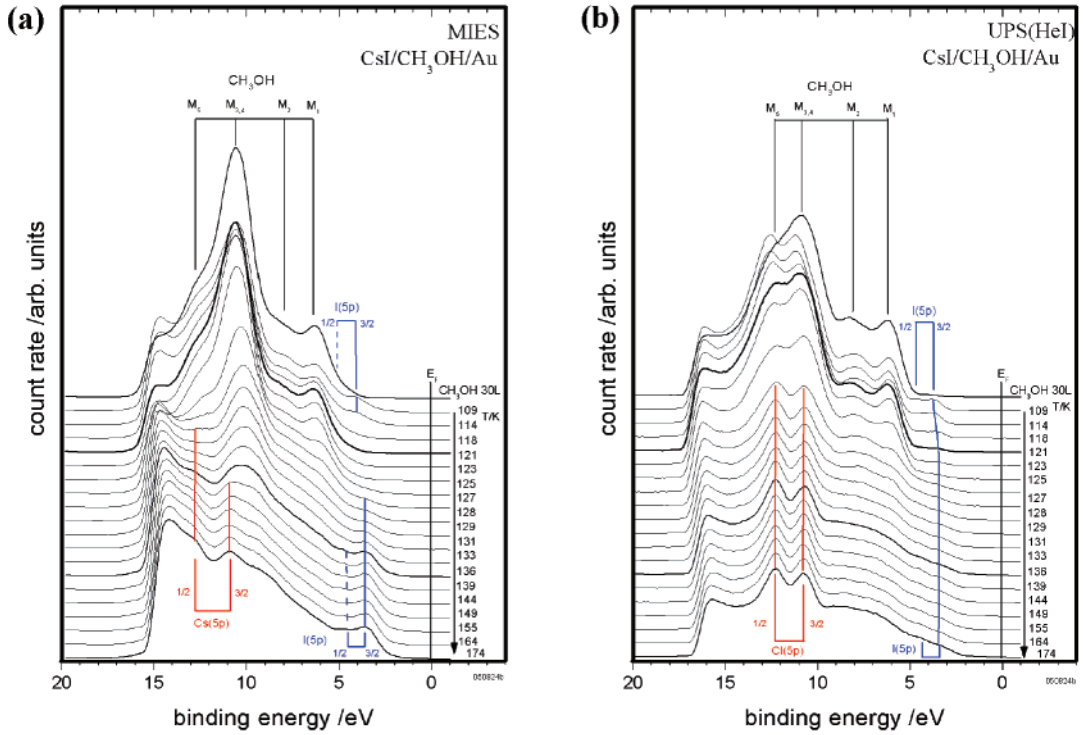

Figure 2. (a) MIES and (b) UPS(HeI) spectra for CsI interacting with amorphous solid methanol. Shown are the spectra of the methanol film prior and after the CsI deposition at about 100 K (upper part) and during the variation of the film temperature between 106 and 174 K (lower part).

and disappearance of Cs(5p) MIES signals (Figure 3). Further annealing is followed by the disappearance of the H_2O spectral features and a regrowth of the iodide signal during the water desorption. At the same time, the Cs(5p) signal reappears during the H_2O desorption (multilayer desorption occurs at 126 K under the present conditions). Similar temperature dependence of the cesium and iodide emission can be noticed in UPS (Figure 1b); however, the intensity variation of I(5p) and Cs(5p) is much less pronounced than in MIES. We have checked that the results displayed below in Figure 3 do not change when the ramping time is further increased. Thus, the chosen ramping time guarantees that thermal equilibrium is present during the annealing procedure. Combining the MIES and UPS results, we can state that, on the laboratory time scale, no H_2O desorption takes place before the minimum in the I(5p) signal is reached (Figure 3).

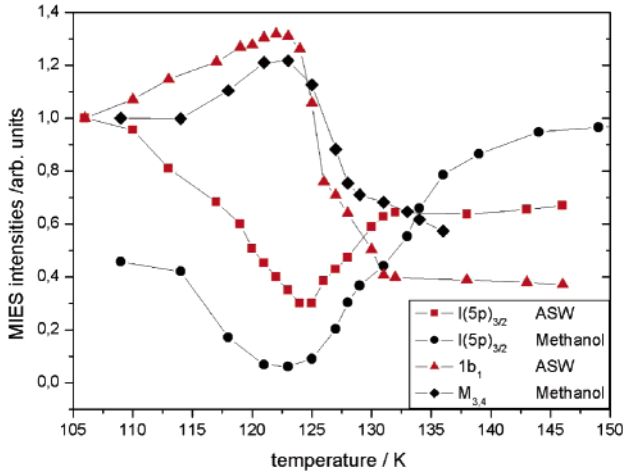

Figure 3. MIES intensities of the spectral features I(5p) and $1b_1$ H_2O (amorphous solid water) and I(5p) and $M_{3,4}$ (amorphous solid methanol) as functions of temperature, after preparation at 100 K.

The most important among the above results is that in MIES, which probes only the top surface layer, the I(5p) signal cannot be made to disappear during annealing but persists over the entire temperature range. This shows directly that iodide never becomes fully solvated, remaining always accessible to the He* probe atoms. In contrary, the Cs(5p) signal disappears in MIES during annealing; i.e., cesium becomes fully solvated, therefore being inaccessible to He*. It is illuminating to compare the present findings for CsI with our results for CsF interacting with ASW, reported recently.[21] Co-deposition of CsF and H_2O (stoichiometry of CsF * 8 H_2O) at 120 K produced a mixed film and, as evidenced by the complete disappearance of both Cs and F features from the MIES (but not UPS) spectra, both cesium and fluoride become fully solvated. This holds true also for the ions close to the surface, which retain their complete solvation shells.[21] The persisting strong UPS signal points to the high solubility of salts in ASW, a property characteristic of liquid water but not of ice.[35]

To obtain information on the accessible surface area of iodide from the present MIES results, we proceeded as follows: we monitored the decrease of the H_2O $1b_1$ signal during the CsI deposition, followed by heating of the sample up to 125 K, a temperature high enough to guarantee that the ionic species Cs^+ and I^- can enter the ASW film. As pointed out above, we have made sure, by an appropriate choice of the temperature ramp, that thermodynamic equilibrium is present during the annealing procedure on the time scale of the experiment. We assume furthermore that thermodynamic equilibrium is reached at 125 K (where the signal I(5p) is minimal) on the time scale of the experiment. We can then estimate that roughly 20% of the surface of the film (with stoichiometry CsI * 32 H_2O) is occupied by iodide ions (which corresponds to 1.7 M when considering the ASW film, exposed to CsI, as a homogeneous solution at 125 K). At that stage, virtually no Cs cations are accessed by the He* probe atoms.

Results similar to those for CsI have been obtained also for the NaI−ASW system. As in the former case, iodide exhibits a strong surface propensity. However, because of the limited potential energy of the He* metastable atoms and the HeI photons, the 2pNa state cannot be ionized; therefore, no information is obtained for the sodium cation.

A significantly different surface behavior from that of ASW is observed when a film of amorphous solid methanol, exposed to CsI, is annealed (Figures 2 and 3). Initially, MIES of the "as-prepared" CsI−methanol film displays the I(5p) structure; however, when annealed above 114 K, the iodide signal starts to disappear (Figure 2a). The I(5p) signal then reappears during further annealing of the film as soon as methanol starts to desorb (i.e., above 130 K). Apparently, iodide becomes fully solvated and not directly exposed at the surface during the initial phase of the annealing, before its MIES signal reappears as a consequence of methanol desorption. It is difficult to judge whether the Cs(5p) signal is seen at all in MIES after CsI exposure at 110 K, due to the strong overlap of Cs(5p) with the methanol $M_{3,4}$ and M_5 features. A similar temperature dependence of the spectral features can be noticed in UPS (Figure 2b); however, the intensity variation of I(5p) is much less pronounced than in MIES. We find that a larger CsI exposure is required to produce a given I(5p) intensity than for ASW. This is taken as evidence that, even around 110 K, the Cs and I species become to some extent embedded into the MeOH film. The above finding has been taken into account also when normalizing the I(5p) signals displayed in Figure 3.

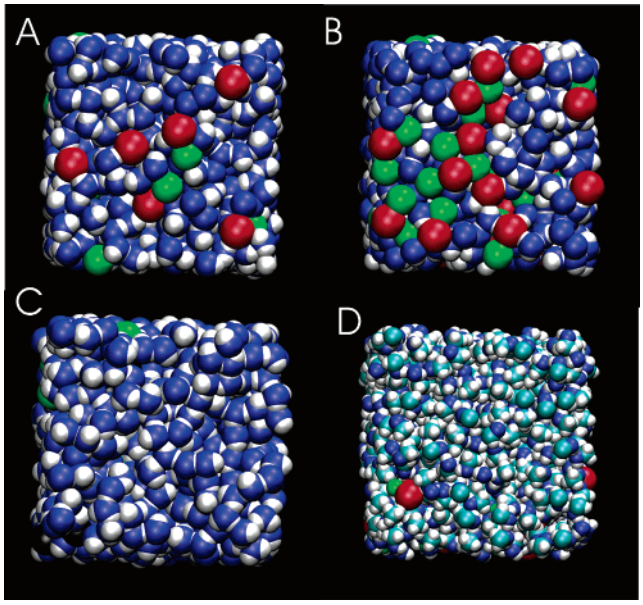

Figure 4. Representative snapshots from molecular dynamics simulations (top views of the slabs) of (a) 1.2 M aqueous CsI, (b) 3 M aqueous CsI, (c) 1.2 M aqueous CsF, and (d) 1.2 M CsI in methanol. Color coding: cesium: green, iodide: red, fluoride: black, oxygen: blue, carbon: cyan, and hydrogen: white.

The methanol-induced feature $M_{3,4}$ appears to be enhanced in MIES compared to UPS. As pointed out above, $M_{3,4}$ is due to the ionization of MOs that are largely localized at the CH_3 group. This indicates that the interfacial methanol molecules are oriented (and remain so also when CsI is supplied) with the methyl groups pointing toward the vacuum, thus being most efficiently accessed by the He* probe atoms.

Computational Results and Comparison with Experiments. The structure of solution/vapor interfaces for CsF or CsI in water and CsI in methanol was investigated by MD simulations. Extended slabs of concentrated liquid solutions, containing a bulk region between two solution/vapor interfaces, were modeled using periodic boundary conditions with a prismatic unit cell. A polarizable force field was employed both for the solvent (water or methanol) and for the Cs^+, F^-, and I^- ions. Nanosecond-length simulations at ambient conditions ensured adequate sampling of structural properties in the interfacial region.

Qualitatively, the principal results of the MD simulations are visualized in Figure 4, which depicts representative snapshots of the surfaces of the four investigated solutions. A clear picture

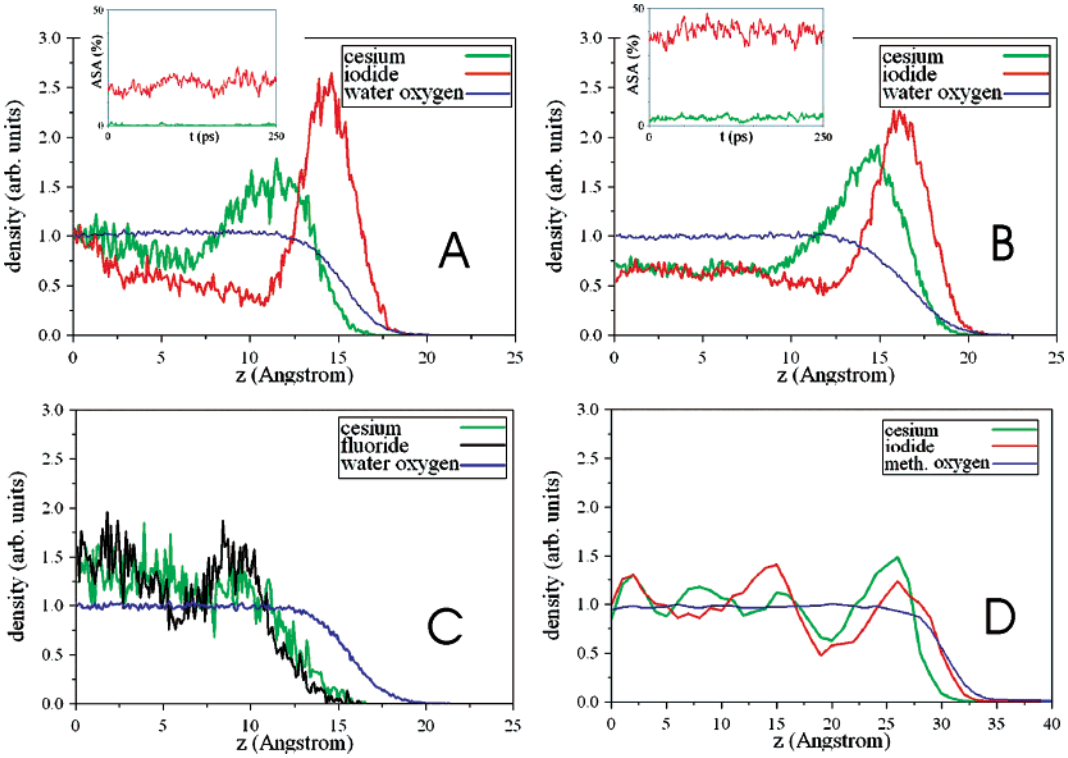

Figure 5. Density profiles (i.e., histogramed densities of the electrolyte ions and solvent molecules in layers parallel to the surface, from the center of the slab across the interface into the gas phase) and accessible surface areas of the individual ionic species (insets) from molecular dynamics simulations of (a) 1.2 M aqueous CsI, (b) 3 M aqueous CsI, (c) 1.2 M aqueous CsF, and (d) 1.2 M CsI in methanol. Accessible surface areas are presented only for cases (a) and (b), where the values are appreciable.

of the surface behavior of the individual ions and solvents emerges already from these snapshots. On one hand, in an aqueous cesium fluoride solution, both cations and anions are repelled from the surface into the bulk, in accord with the standard model of surfaces of electrolytes.[2−4] On the other hand, iodide exhibits a strong propensity for the aqueous surface. At concentrations above roughly 1 M, I^- also tends to drag the Cs^+ counterions toward the surface and strong ion pairing occurs. Unlike in water, none of the investigated ions show any appreciable segregation at the surface of methanol solutions. Clearly, in addition to the surface driving ion and solvent polarizabilities,[6−8] other effects come into play, such as the Coulombic and hydrophobic effects connected with surface orientations of solvent molecules (methanol having surface-exposed methyl groups and water exhibiting dangling hydrogens). The degree of surface segregation of iodide is thus dependent on the nature of the polar solvent with water playing a special role.

The results of the MD simulations are further quantified in Figure 5, which shows the density profiles of the individual ionic species in the two solvents. For CsI in water, we also depict the accessible surface areas (ASA) of the two ionic species. In 1.2 M aqueous CsI, the peak surface enhancement of iodide amounts to roughly 2.5 times the bulk concentration, and it is complemented by subsurface ion depletion. Cs^+ ions are per se repelled from the surface; however, due to charge neutralization, they tend to accumulate in the subsurface, creating effectively an electric double layer. The ASA analysis reveals that at this concentration, roughly 16% of the surface is occupied by iodide anions, whereas virtually no cesium cations are directly exposed into the gas phase (Figure 5a), which is in quantitative agreement with the above MIES results. Upon increasing the CsI concentration to 3 M, the importance of the attractive anion−cation interactions is further enhanced. As a result, the cesium and iodide density peaks move closer to each other, the former being shifted closer to the surface, and the latter slightly decreasing in height. Consistently, the ASA of iodide grows slightly sublinearly with salt concentration reaching roughly 40% at 3 M, with the ASA of cesium being only a few percent (Figure 5b).

The situation changes dramatically upon switching the anion from iodide to fluoride or the solvent from water to methanol. The density profiles in a 1.2 M aqueous CsF solution show that all ions are repelled from the surface, leaving an ion-free surface-water layer of a thickness of about 3 Å (Figure 5c). Interestingly, Cs^+ penetrates slightly closer to the interface than F^-, which indicates a reversed polarity of the electric double layer compared to aqueous alkali iodide solutions, in agreement with previous measurements.[4]

The density profiles show quantitatively that the surface propensity of iodide for the methanol surface is dramatically reduced compared to that in water (Figure 5d). As a matter of fact, there is virtually no surface enhancement of iodide at the methanol surface, and the iodide density profile more or less matches that of water with a little bit of oscillation within the interface. A close inspection of the surface structures reveals that the interfacial iodide ions are significantly less frequent and more buried in methanol than in the case of water, not being directly exposed from the vapor side. In methanol, the cesium signal follows that of iodide, exhibiting, however, a slight shift toward the bulk. In summary, the MD simulations of surfaces of salt solutions fully support the experimental results for the corresponding amorphous solids.

Conclusions

Present MIES experiments point directly to segregation of salt ions at aqueous surfaces. Whereas previous spectroscopic

measurements of liquid solutions probed the whole solution/vapor interface,[12−16] MIES gives information about the structure of the topmost layer and can straightforwardly distinguish whether an ion is exposed to the gas phase or not. The surface propensity is ion specific (being present for iodide but not for fluoride or cesium) and virtually vanishes in amorphous solid methanol.

The experimental results on amorphous solid water and methanol surfaces are in quantitative agreement with predictions from molecular dynamics simulations for surfaces of liquid aqueous and methanol solutions of CsF and CsI salts. On one hand, the present study provides strong evidence for the remarkable ability of water to surface segregate heavier halide anions, which has direct implications for atmospheric processes at aqueous aerosols and for heterogeneous chemistry in general. On the other hand, present results support previous claims[19] that solvation processes take place in the same way at surfaces of amorphous solids (water or methanol) as at the surfaces of the corresponding liquids, albeit on a vastly prolonged time scale (seconds as compared to picoseconds).

Acknowledgment. Support from the Czech Ministry of Education (Grants LC512 and ME644) and via the NSF-funded Environmental Molecular Science Institute (Grants CHE 0431312 and 0209719) is gratefully acknowledged. The work at PNNL was performed under the auspices of the Division of Chemical Sciences, Office of Basic Energy Sciences, U.S. Department of Energy.

References and Notes

(1) Buch, V.; Devlin, J. P.; Eds. *Water in Confining Geometries*; Springer: Berlin, 2002.

(2) Onsager, L.; Samaras, N. N. T. *J. Chem. Phys.* **1934**, *2*, 528.

(3) Adam, N. K. *The Physics and Chemistry of Surfaces*; Oxford University Press: London, 1941.

(4) Randles, J. E. B. *Phys. Chem. Liq.* **1977**, *7*, 107.

(5) Knipping, E. M.; Lakin, M. J.; Foster, K. L.; Jungwirth, P.; Tobias, D. J.; Gerber, R. B.; Dabdub, D.; Finlayson-Pitts, B. J. *Science* **2000**, *288*, 301.

(6) Jungwirth, P.; Tobias, D. J. *J. Phys. Chem. B* **2001**, *105*, 10468.

(7) Dang, L. X.; Chang, T.-M. *J. Phys. Chem. B* **2002**, *106*, 235.

(8) Jungwirth, P.; Tobias, D. J. *J. Phys. Chem. B* **2002**, *106*, 6361.

(9) Archontis, G.; Leontidis, E.; Andreou, G. *J. Phys. Chem. B* **2005**, *109*, 17957.

(10) Hu, J. H.; Shi, Q.; Davidovits, P.; Worsnop, D. R.; Zahniser, M. S.; Kolb, C. E. *J. Phys. Chem.* **1995**, *99*, 8768.

(11) Finlayson-Pitts, B. J. *Chem. Rev.* **2003**, *103*, 4801.

(12) Petersen, P. B.; Johnson, J. C.; Knutsen, K. P.; Saykally, R. J. *Chem. Phys. Lett.* **2004**, *397*, 46.

(13) Liu, D.; Ma, G.; Levering, L. M.; Allen, H. C. *J. Phys. Chem. B* **2004**, *108*, 2252.

(14) Raymond, E. A.; Richmond, G. L. *J. Phys. Chem. B* **2004**, *108*, 5051.

(15) Ghosal, S.; Hemminger, J. C.; Bluhm, H.; Mun, B. S.; Hebenstreit, E. L. D.; Ketteler, G.; Ogletree, D. F.; Requejo, F. G.; Salmeron, M. *Science* **2005**, *307*, 563.

(16) Weber, R.; Winter, B.; Schmidt, P. M.; Widdra, W.; Hertel, I. V.; Dittmar, M.; Faubel, M. *J. Phys. Chem. B* **2004**, *108*, 4729.

(17) The News Staff, *Science* **2004**, *306*, 2017.

(18) Kimmel, G. A.; Stevenson, K. P.; Dohnalek, Z.; Smith, R. S.; Kay; B. D. *J. Chem. Phys.* **2001**, *114*, 5284.

(19) Garrett, B. C.; Dixon, D. A.; Camaioni, D. M.; Chipman, D. M.; Johnson, M. A.; Jonah, C. D.; Kimmel, G. A.; Miller, J. H.; Rescigno, T. N.; Rossky, P. J.; Xantheas, S. S.; Colson, S. D.; Laufer, A. H.; Ray, D.; Barbara, P. F.; Bartels, D. M.; Becker, K. H.; Bowen, K. H. Jr.; Bradforth, S. E.; Carmichael, I.; Coe, J. V.; Corrales, L. R.; Cowin, J. P.; Dupuis, M.; Eisenthal, K. B.; Franz, J. A.; Gutowski, M. S.; Jordan, K. D.; Kay, B. D.; LaVerne, J. A.; Lymar, S. V.; Madey, T. E.; McCurdy, C. W.; Meisel, D.; Mukamel, S.; Nilsson, A. R.; Orlando, T. M.; Petrik, N. G.; Pimblott, S. M.; Rustad, J. R.; Schenter, G. K.; Singer, S. S.; Tokmakoff, A.; Wang, L.-S., Wittig, C.; Zwier, T. S. *Chem. Rev.* **2005**, *105*, 355.

(20) Lucas, S.; Ferry, D.; Demirdjian, B.; Suzanne, J. *J. Phys. Chem. B* **2005**, *109*, 18103.

(21) Borodin, A.; Höfft, O.; Kempter, V. *J. Phys. Chem. B* **2005**, *109*, 16017.

(22) Kim, J. H.; Shin, T.; Jung, K.-H.; Kang, H. *ChemPhysChem* **2005**, *6*, 440.

(23) Souda, R. *J. Phys. Chem. B* **2005**, *109*, 21879.

(24) Borodin, A.; Höfft, O.; Kahnert, U.; Kempter, V.; Ferro, Y.; Allouche, A. *J. Chem. Phys.* **2004**, *120*, 8692.

(25) Morgner, H. *Adv. At. Mol. Opt. Phys.* **2000**, *42*, 387.

(26) Harada, H.; Masuda, S.; Osaki, H. *Chem. Rev.* **1997**, *97*, 1897.

(27) *)* Case, D. A.; Pearlman, D. A.; Caldwell, J. W.; Cheatham, T. E., III; Ross, W. S.; Simmerling, C. L.; Darden, T. A.; Merz, K. M.; Stanton, R. V.; Cheng, A. L.; Vincent, J. J.; Crowley, M.; Tsui, M.; Radmer, R. J.; Duan, R. Y.; Pitera, J.; Massova, I.; Seibel, G. L.; Singh, U. C. *AMBER6*; University of California, San Francisco, 1999.

(28) Caldwell, J. W.; Kollman, P. A. *J. Phys. Chem.* **1995**, *99*, 6208.

(29) Dang, L. X. *J. Phys. Chem. B* **1999**, *103*, 8195.

(30) Dang, L. X. *J. Phys. Chem. B* **2002**, *106*, 10388.

(31) Essmann, U.; Perera, L.; Berkowitz, M. L.; Darden, T.; Pedersen, L. G. *J. Chem. Phys.* **1995**, *103*, 8577.

(32) Ryckaert, J.-P.; Ciccotti, G.; Berendsen, H. J. C *J. Comput. Phys.* **1977**, *23*, 327.

(33) Dang, L. X. *J. Phys. Chem. A* **2004**, *108*, 9014.

(34) Günster, J.; Krischok, S.; Kempter, V.; Stultz, J.; Goodman, D. W. *Surf. Rev. Lett.* **2002**, *9*, 1511.

(35) Petrenko, V. F.; Whitworth, R. W. *Physics of Ice*; Oxford University Press: Oxford, 1999.